Available online at www.sciencedirect.com
ScienceDirect
International Journal of Heat and Mass Transfer 50 (2007) 3422–3436
International Journal of HEAT and MASS TRANSFER
www.elsevier.com/locate/ijhmt

Boundary conditions at a fluid–porous interface: An *a priori* estimation of the stress jump coefficients

M. Chandesris, D. Jamet *

Laboratoire de Modélisation et de Développement de Logiciels, DEN/DER/SSTH, CEA Grenoble, 17 rue des Martyrs, 38054 Grenoble Cedex 9, France

Received 22 March 2006; received in revised form 7 January 2007
Available online 11 April 2007

Abstract

The momentum transfer at the interface between a porous medium and an adjacent free fluid is investigated by introducing three different levels of description of the problem. This study focuses mainly on the up-scaling from the mesoscopic to the macroscopic level of description. An explicit relation between the jump parameters, the location of the discontinuous interface (macroscopic description) and the structure of the transition region (mesoscopic description) is obtained. This relation allows to explain the large sensitivity of the jump parameters to the location of the discontinuous interface observed in previous studies. It is shown that it is crucial to conserve *exactly* the forces in the up-scaling analysis.

Keywords: Interface; Excess quantity; Boundary conditions; Porous media

1. Introduction

The problem of momentum transfer at the interface between a porous medium and an adjacent free fluid has been the object of considerable attention. Indeed, transport phenomena at a fluid–porous interface are encountered in a wide range of technological applications (packed-bed heat exchangers, nuclear waste repositories, drying processes, *etc.*), or in environmental sciences (flows in rivers, ground-water pollution, flows over plant canopies, *etc.*). The understanding of the momentum transfer at a fluid–porous interface is crucial for the development of accurate models in which other transfers are involved such as heat, pollutants, oxide and carbon dioxide, passive solute, *etc*.

To study the fluid–porous interfacial region, three different levels of description can be considered. At the *microscopic* scale, the flow in the entire fluid domain (free fluid region and pores of the porous medium) is governed by the well-known Navier–Stokes equations. However, for most practical applications, it is not possible to compute the flow in the entire fluid domain. The cost and the present-day computer capacity are the first restrictions. Furthermore, except for porous media with a simple structure, it is generally impossible to exactly describe the porous medium at this scale due to its high local heterogeneity. Thus, the study of this problem requires to introduce other levels of description. At the *mesoscopic* scale, the fluid and solid phases are replaced by a single equivalent medium. This is the basis of the continuum approach for flows in porous media. At this continuous level, the zone located in between the two homogeneous regions (*i.e.* porous medium and free fluid), is a continuous heterogeneous transition zone, where the properties of the medium (*e.g.* porosity) encounter strong but nevertheless continuous variations. Finally, at the *macroscopic* scale, the system is characterized by two homogeneous regions, separated by an interface of discontinuity. This macroscopic scale description requires to specify boundary conditions at the interface between the two homogeneous media. These three different levels of description are illustrated in Fig. 1.

* Corresponding author. Tel.: +33 (0) 4 38 78 45 42; fax: +33 (0) 4 38 78 51 95.
E-mail address: didier.jamet@cea.fr (D. Jamet).

0017-9310/$ - see front matter © 2007 Elsevier Ltd. All rights reserved.
doi:10.1016/j.ijheatmasstransfer.2007.01.053

Nomenclature

d_p	size of a small cube (DNS simulation)
h	height of the fluid channel
h_b	height of the porous medium
K	permeability
K_p	permeability of the homogeneous porous medium
p	pressure
u	velocity
u_A	solution of the matched asymptotic analysis
u_B	slip velocity
u_c	solution at the mesoscopic scale
u_d	solution at the macroscopic scale
U_D	Darcy velocity
U_∞	asymptotic value of the velocity in the porous medium as $y \to -\infty$
y_i	arbitrary position in the transition zone
y_M	location of the discontinuous interface
y_ψ	location of the center of gravity of the variable ψ
y_{imp}	location of the equivalent impermeable wall

Special symbols

$\langle\psi\rangle$	volumetric average (or phase average)
$\langle\psi\rangle_f$	intrinsic phase average

Greek symbols

α	slip coefficient of Beavers and Joseph [1]
β	stress jump coefficient of Ochoa-Tapia and Whitaker [15]
δ	thickness of the boundary region
Δy	difference between the center of gravity of the friction surface-excess force and $y_{\phi/K}$
ϵ	δ/h, small parameter
ϕ	porosity
ϕ_p	porosity of the homogeneous porous medium
μ	viscosity of the fluid
μ_{eff}	effective viscosity of the fluid in the porous medium

Superscripts

$\psi^\star$	non-dimensional variable
$\bar{\psi}$	*inner* variable
ψ^{ex}	first definition of the excess quantity
ψ^{exM}	second definition of the excess quantity
$\psi^{ex\Delta}$	third definition of the excess quantity

Subscripts

ψ_+, ψ_-	constant asymptotic values of ψ outside the transition zone

The last level of description (*i.e.* macroscopic scale) is the most commonly used for the study of practical applications. The main difficulty, when working at this level of description, is the specification of appropriate boundary conditions that must be applied at the interface. Beavers and Joseph [1] have shown that the wall permeability implies a non-zero velocity at the interface, *i.e.* an apparent slip velocity. They have proposed a semi-empirical slip boundary condition

$$\left.\frac{du}{dy}\right|_{y=0} = \frac{\alpha}{\sqrt{K_p}}(u_B - U_D) \tag{1}$$

that allows a non-zero velocity at the interface. Here, $y = 0$ is the location of the interface, $u_B = \langle u\rangle|_{y=0}$ is the free fluid velocity at the interface, U_D is the Darcy velocity inside the porous medium, K_p is the permeability of the porous medium and α is a dimensionless coefficient. The values of α are adjusted to obtain good agreement with the experimental data they provided [1]. Other studies have focused on the determination of this coefficient. It has been found that this coefficient strongly depends on the geometry of the transition region [2,21,17]. Furthermore, following different approaches, Larson and Higdon [10,11], Sahraoui and Kaviany [19] and Saffman [18] have shown that the value of α depends strongly on the exact location of the interface of discontinuity. However, no agreement on a best choice for the determination of the exact location of this interface of discontinuity inside the transition region has been reached.

In [1], Beavers and Joseph used the Darcy's law to describe the flow in the porous medium. Since Darcy's law does not allow to describe any boundary layer region within the porous region close to the interface, Neale and Nader [13] proposed to use instead the Darcy-Brinkman equation in the porous medium

$$\mu_{eff}\frac{d^2\langle u\rangle}{dy^2} - \frac{\mu}{K_p}\langle u\rangle = \frac{d\langle p\rangle_f}{dx} \tag{2}$$

where μ_{eff} is the effective viscosity of the fluid in the porous medium. Assuming continuity of both the velocity and stress (built on the effective viscosity) at the interface, they obtained a solution identical to that of Beavers and Joseph [1] in the free fluid region provided that $\alpha = \sqrt{\mu_{eff}/\mu}$. The advantage of this approach appears clearly in situations where it is important to describe the boundary layer within the porous region. However, this approach has several limitations. First, it is still not possible to predict the effective viscosity μ_{eff} of a given porous medium. Second, as stressed

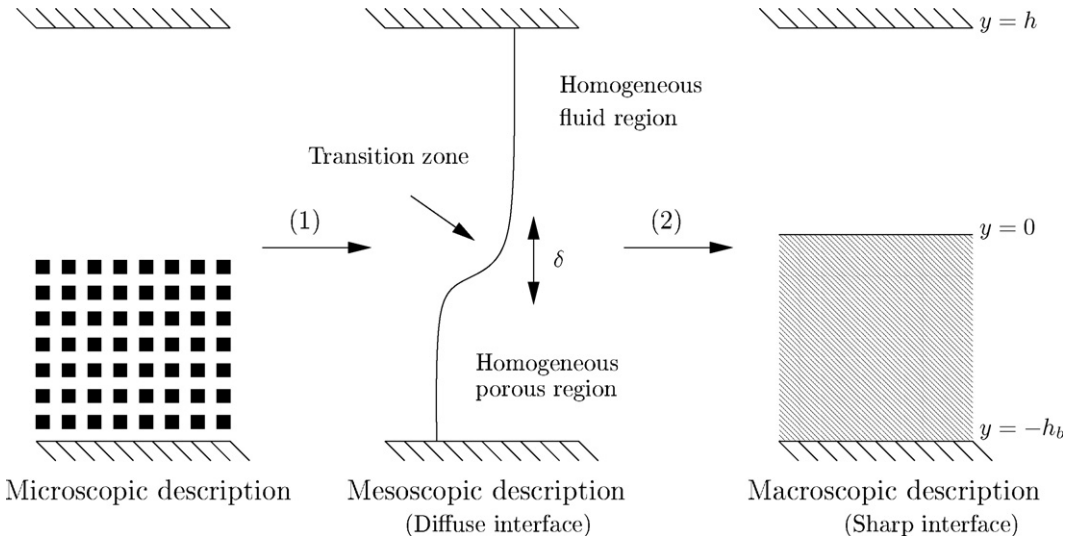

Fig. 1. The three different scales of description of a porous/fluid transition.

out by Nield [14], if the hypothesis of continuity of both the velocity and stress is clearly valid at the microscopic level (in the pores), nothing indicates that it is still valid at the macroscopic level of description. Finally, the result is still extremely sensitive to the exact location of the discontinuous interface.

More recently, a very interesting approach to develop appropriate jump conditions for the momentum transport at the interface has been proposed by Ochoa-Tapia and Whitaker [15,16]. In their work, they propose two modeling steps. The first one allows to go from the microscopic description of the problem to the mesoscopic scale, using the volume-averaging method. At this mesoscopic level, a single volume-averaged transport equation is valid everywhere: in the two homogeneous regions as well as in the heterogeneous transition zone. Then, in a second step, they propose a method to derive jump conditions at the macroscopic scale of description, starting from the continuous approach of the mesoscopic scale of description. The structure of their theory is comparable to that used to develop jump conditions at fluid–fluid interfaces. An introduction to this theory can be found in [7]. They obtain the following stress jump condition:

$$\left.\frac{\mathrm{d}\langle u\rangle}{\mathrm{d}y}\right|_{y=0^+} - \frac{1}{\phi_\mathrm{p}}\left.\frac{\mathrm{d}\langle u\rangle}{\mathrm{d}y}\right|_{y=0^-} = -\frac{\beta}{\sqrt{K_\mathrm{p}}}\langle u\rangle|_{y=0} \tag{3}$$

where ϕ_p is the porosity of the homogeneous porous medium and β is a dimensionless parameter of the order of one. As for the α coefficient, good agreement with the experimental data of Beavers and Joseph [1] is obtained only by adjusting the values of this parameter. Indeed, in their analysis, β is a very complex function that depends on the representations of several surface excess quantities, whose values are unknown. It has to be noticed that the derivation of the closure problem associated to the determination of this parameter still remains a challenge [9].

Ochoa-Tapia and Whitaker [15] do not provide an explicit relation between β and the structure of the transition region. However, they propose [16] a first numerical attempt to determine the value of β by solving numerically a variable porosity model in the transition zone. Unfortunately, their attempt is not successful. Since the practical use of the jump conditions (3) requires the specification of the value of β, other studies are focusing on its determination [9,12,6]. The comparisons of different numerical approaches, followed by Min and Kim [12] and by Deng and Martinez [6], do not allow to understand the physical origin of the jump parameter β, nor to relate its value to the structure of the porous medium close to the interface. By introducing a heterogeneous continuously varying transition zone between the porous region and the free-fluid region, Goyeau et al. [9] obtain an explicit function for the stress jump coefficient β. They are the firsts to exhibit an analytic dependence of β to the continuous variations of the porous structure. However, the expression proposed for β is not closed, since it still depends on the unknown velocity inside the transition zone. As they point out, further studies are needed toward the exact determination of β.

The two-step modeling approach introduced by Ochoa-Tapia and Whitaker [15] is, from our point of view, very relevant for the study of interfacial phenomena. In the second step of their analysis, Ochoa-Tapia and Whitaker [15] only suggest general representations to evaluate the difference between mesoscopic and macroscopic quantities in the heterogeneous transition region. Recently, Chandesris and Jamet [5] have shown that, given a single volume-averaged transport equation in the entire domain (mesoscopic scale), it is possible to solve the problem analytically inside the heterogeneous transition zone using the method of matched asymptotic expansions and thus to analytically derive the boundary conditions that must be applied at the discontinuous interface. This analytical study shows

that the stress jump condition is related to the slip velocity but also to the pressure gradient, through two jump parameters. This analysis also provides explicit relations between these two jump parameters and the variations of the porosity and permeability in the transition zone. This dependence is expressed through two excess quantities. In [5], the values of these excess quantities are adjusted to obtain good agreement with the experimental data of Beavers and Joseph [1], since the exact permeability and porosity profiles of the materials used in these experiments are not available. However, since this analysis directly relates the excess quantities to the variations of the porosity and permeability in the transition zone, it should be possible to evaluate *a priori* the values of these excess quantities for the surface of a given material, provided that the porosity and permeability profiles are known in the transition zone. The objective of the present study is to confirm this last point.

This article is organized as follows. The second section briefly recalls the theoretical aspects and the results of the analytical study presented in [5]. The third section focuses on the definition and properties of the excess quantities. The linear dependence of the value of the excess quantities on the location of the discontinuous interface is highlighted. Then, the determination of the porosity and permeability profiles at the mesoscopic level, that are needed to make a full comparison, is addressed. In the fourth section, the *a priori* evaluation of the excess quantities is studied. It is shown that a constraint of conservation should be introduced in the matched asymptotic expansion analysis. Provided that this constraint is satisfied, it is demonstrated that it is possible to evaluate *a priori* the excess quantities. These developments are illustrated in the fifth section by performing comparisons with 1D numerical results.

2. Results obtained with the matched asymptotic expansions

In this section, we briefly recall the system studied in [5], the main ideas of the method of matched asymptotic expansions as well as the results that were obtained. Let us consider the classical system sketched in Fig. 1 made of a two-dimensional channel bounded by a permeable lower wall and an impermeable upper wall. We consider that the flow parallel to the channel is incompressible and laminar. At the mesoscopic level of description, the flow in the entire domain is modeled using a variable permeability and porosity model:

$$\frac{\mathrm{d}^2\langle u\rangle}{\mathrm{d}y^2} = \frac{\phi(y)}{K(y)}\langle u\rangle + \frac{\phi(y)}{\mu}\frac{\mathrm{d}\langle p\rangle_\mathrm{f}}{\mathrm{d}x} \tag{4}$$

where $\langle\cdot\rangle$ is the *phase average* operator (or volumetric average) defined by [22]:

$$\langle\psi\rangle = \frac{1}{V}\int_{V_\mathrm{f}} \psi\,\mathrm{d}V \tag{5}$$

for any physical variable ψ, where V_f represents the volume of the fluid phase contained within the averaging volume V, while $\langle\cdot\rangle_\mathrm{f}$ is the *intrinsic phase average* operator defined by:

$$\langle\psi\rangle_\mathrm{f} = \frac{1}{V_\mathrm{f}}\int_{V_\mathrm{f}} \psi\,\mathrm{d}V \tag{6}$$

These two averages are related through the porosity ϕ by:

$$\langle\psi\rangle = \phi\langle\psi\rangle_\mathrm{f}, \quad \phi = \frac{V_\mathrm{f}}{V} \tag{7}$$

To solve this problem, the matched asymptotic expansions method is used (*e.g.* [23,24]). This method is applicable to the resolution of differential equations in which a small parameter ϵ is present. It consists in dividing the resolution domain in a set of sub-regions: two *outer regions*, where the variables of the system are slowly varying, and an *inner region*, where these variables are rapidly varying. A change of variable is introduced in the inner region. The problem is solved separately in each region using an asymptotic expansion in ϵ. At first order, in the outer regions, the solution is sought for in the following form:

$$\langle u\rangle(y,\epsilon) = \langle u\rangle^{(0)}(y) + \epsilon\langle u\rangle^{(1)}(y) + \mathcal{O}(\epsilon^2) \tag{8}$$

Then, matching relations are used to match the solutions of the inner and outer regions. Chandesris and Jamet [5] apply this method to the resolution of Eq. (4) where the small parameter ϵ is the ratio δ/h; δ is the thickness of the heterogeneous transition region and h is the height of the free channel (see Fig. 1). This small parameter is present in the porosity and permeability profiles. The result obtained at first order in [5] for the velocity is noted $u_\mathrm{A} = \langle u\rangle^{(0)} + \epsilon\langle u\rangle^{(1)}$ and is the solution of the following problem:

$$\frac{\mathrm{d}^2 u_\mathrm{A}}{\mathrm{d}y^2} = \frac{1}{\mu}\frac{\mathrm{d}\langle p\rangle_\mathrm{f}}{\mathrm{d}x}, \quad 0 \leqslant y \leqslant h \tag{9}$$

$$\frac{\mathrm{d}^2 u_\mathrm{A}}{\mathrm{d}y^2} - \frac{\phi_\mathrm{p}}{K_\mathrm{p}}u_\mathrm{A} = \frac{\phi_\mathrm{p}}{\mu}\frac{\mathrm{d}\langle p\rangle_\mathrm{f}}{\mathrm{d}x}, \quad y \leqslant 0 \tag{10}$$

At zeroth order, the velocity $\langle u\rangle^{(0)}$ and its gradient are continuous at the interface [5]. At first order, the following jump conditions are obtained for u_A:

$$u_\mathrm{A}|_{y=0^+} - u_\mathrm{A}|_{y=0^-} = 0 \tag{11}$$

$$\left.\frac{\mathrm{d}u_\mathrm{A}}{\mathrm{d}y}\right|_{y=0^+} - \left.\frac{\mathrm{d}u_\mathrm{A}}{\mathrm{d}y}\right|_{y=0^-} = \frac{\delta}{K_\mathrm{p}}\left(\frac{\bar{\phi}^\star}{\bar{K}^\star}\right)^{\mathrm{ex}}\langle u\rangle^{(0)}|_{y=0} + \frac{\delta}{\mu}(\bar{\phi}^\star)^{\mathrm{ex}}\frac{\mathrm{d}\langle p\rangle_\mathrm{f}}{\mathrm{d}x} \tag{12}$$

where the superscript * denotes a non-dimensional variable:

$$K^\star \hat{=} \frac{K}{K_\mathrm{p}}, \quad \phi^\star \hat{=} \phi, \quad y^\star \hat{=} \frac{y}{h} \tag{13}$$

and the overbar a variable inside the inner region:

$$\bar{f}(\bar{y}^\star) \hat{=} f\left(\frac{y^\star}{\epsilon}\right) \tag{14}$$

It should be noticed that the stress jump condition at first order (12) depends on the knowledge of the velocity at zeroth order $\langle u\rangle^{(0)}$. Therefore, to obtain the solution u_A, the system has to be solved in two steps: first the zeroth order term $\langle u\rangle^{(0)}$ which is the solution of Eqs. (9) and (10) with continuous velocity and velocity gradient at the interface, then the first order term u_A which is a better approximation since it is the solution of the same problem however with a different and physically more relevant jump condition. In Eq. (12), the excess quantity ψ^{ex} of any physical variable ψ is defined by:

$$\psi^{ex} \hat{=} y_i(\psi_- - \psi_+) + \int_{-\infty}^{y_i}(\psi - \psi_-) + \int_{y_i}^{+\infty}(\psi - \psi_+) \tag{15}$$

where y_i is an *arbitrary* position inside the heterogeneous transition zone and $\psi_\pm$ are the constant asymptotic values of ψ outside the heterogeneous transition zone. It is worth noticing that the excess quantity ψ^{ex} is independent of the choice of y_i. The changes of variables (13) and (14) and the definition of the excess quantities imply the following relations:

$$\frac{\delta}{K_p}\left(\frac{\bar{\phi}^\star}{\bar{K}^\star}\right)^{ex} = \left(\frac{\phi}{K}\right)^{ex}, \quad \delta\left(\bar{\phi}^\star\right)^{ex} = (\phi)^{ex} \tag{16}$$

Thus the stress jump condition (12) for u_A is simply given by:

$$\left.\frac{du_A}{dy}\right|_{y=0^+} - \left.\frac{du_A}{dy}\right|_{y=0^-} = \left(\frac{\phi}{K}\right)^{ex}\langle u\rangle^{(0)}|_{y=0} + \frac{1}{\mu}(\phi)^{ex}\frac{d\langle p\rangle_f}{dx} \tag{17}$$

This shows that the specification of the value of δ is unnecessary. This information is indirectly contained in the excess quantities $(\phi/K)^{ex}$ and $(\phi)^{ex}$ whose numerical values depend only on the porosity and permeability profiles in the transition zone.

2.1. Definition of the macroscopic problems

The matched asymptotic expansion (MAE) analysis shows that the solution at first order in ϵ of the *mesoscopic* problem given by Eq. (4) is the solution of a *macroscopic* problem defined by Eqs. (9)–(11) and (17). This system is characterized by two regions with constant properties, separated by an interface of discontinuity and should be equivalent to the *mesoscopic* problem. However, since the stress jump condition (17) depends on the knowledge of the velocity at zeroth order, this macroscopic problem has to be solved in two steps. Thus, this macroscopic problem might not be the most appropriate for the study of practical applications. To overcome this difficulty and to simplify the resolution of this problem, one could choose to replace the zeroth order velocity $\langle u\rangle^{(0)}$ of Eq. (17) by the "total" velocity $\langle u\rangle$:

$$\left.\frac{d\langle u\rangle}{dy}\right|_{y=0^+} - \left.\frac{d\langle u\rangle}{dy}\right|_{y=0^-} = \left(\frac{\phi}{K}\right)^{ex}\langle u\rangle|_{y=0} + \frac{1}{\mu}(\phi)^{ex}\frac{d\langle p\rangle_f}{dx} \tag{18}$$

Indeed, in this case, the *macroscopic* problem defined by Eqs. (9)–(11) and (18) can be solved in one step. However, the consequences of the substitution of $\langle u\rangle^{(0)}$ by $\langle u\rangle$ in the stress jump condition might be important and have to be carefully studied before being used. To distinguish between these two macroscopic problems, the problem defined using the jump condition (17) will be called the MAE macroscopic problem, whereas the problem defined using the jump condition (18) will be called the one step (OS) macroscopic problem.

3. Definition and properties of the excess quantities

3.1. Dependence on the location of the discontinuous interface

It has to be noticed that the definition of the excess quantity given by Eq. (15) assumes that the discontinuous interface is located at $y = 0$. Indeed, the analytical study has been carried out in [5] using the matched asymptotic expansions around the position $y = 0$. However, other choices could have been made to locate the interface of discontinuity inside the transition region since this region is continuous. Thus, to keep as much generality as possible, we now assume that the interface of discontinuity is located at $y = y_M$, without specifying *a priori* this location. The MAE analysis carried out in [5] can thus be generalized and it is found that the matching conditions are then given by:

$$\lim_{y\to y_M^\pm} f(y,\epsilon) = \lim_{\bar{\zeta}\to\pm\infty}\bar{f}(\bar{\zeta},\epsilon) \tag{19}$$

with $\bar{\zeta} = (y - y_M)/\epsilon$. The stress jump condition (17) is now valid at $y = y_M$ and the excess quantity that appears in the analytical study is given by:

$$\psi^{exM} = (y_i - y_M)(\psi_- - \psi_+) + \int_{-\infty}^{y_i}(\psi - \psi_-) + \int_{y_i}^{+\infty}(\psi - \psi_+) \tag{20}$$

This result is obtained by a simple change of variables. With this new definition, the excess quantity is still independent of the arbitrary choice of y_i. However, the expression (20) shows that the value of the excess quantities *does* depend on the location of the surface of discontinuity y_M. The definition (20) of the excess quantity is illustrated for $y_i = y_M$ in Fig. 2a where the excess quantity is represented by the area of the crosshatched surface.

To simplify the expression (20), a new quantity is now introduced. For any physical quantity ψ, y_ψ is defined as the particular value of y_i such that the sum of the last two integral terms of (20) is zero:

$$\int_{-\infty}^{y_\psi}(\psi - \psi_-) + \int_{y_\psi}^{+\infty}(\psi - \psi_+) = 0 \tag{21}$$

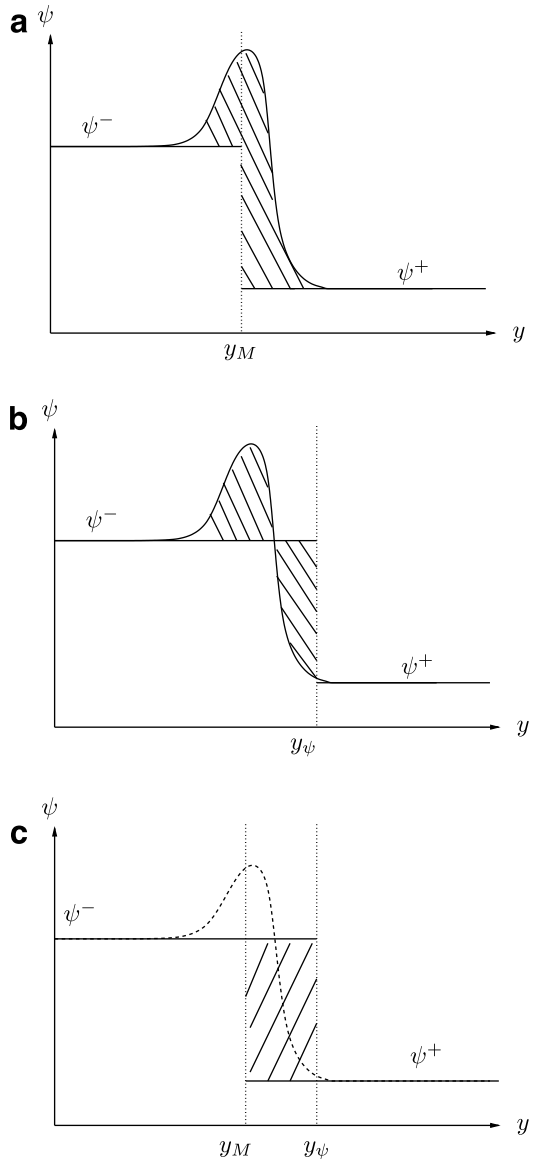

Fig. 2. Different representations of an excess quantity. (a) Excess quantity, (b) definition of y_ψ using Eq. (21), (c) excess quantity given by Eq. (22).

and is therefore named the center of gravity of the profile of ψ. It comes:

$$\psi^{\mathrm{exM}} = (y_\psi - y_{\mathrm{M}})(\psi_- - \psi_+) \tag{22}$$

This definition is illustrated in Fig. 2. y_ψ is such that the two crosshatched areas of Fig. 2b are equal. The new expression (22) giving the excess quantity corresponds to the crosshatched area of Fig. 2c. On these figures, the location of the discontinuous interface y_{M} is arbitrary, while the location of y_ψ is not. As shown by Eq. (21), y_ψ is defined only by the profile of $\psi(y)$. Furthermore, Eq. (22) shows that the dependence of the excess quantity ψ^{exM} is *linear* on y_{M}. This result explains the large sensitivity of the stress jump coefficient with the position of the surface of discontinuity reported in previous studies [18,10,19,4].

3.2. Porosity and permeability profiles

In order to validate our analysis and to determine the numerical values of the excess quantities, we have to specify the porosity and permeability profiles in the heterogeneous transition region. Indeed, these profiles are necessary to compute the flow at the mesoscopic scale and to determine the excess quantities without resorting to adjusted values at the macroscopic scale. Since the objective of this study is not to focus on the determination of these profiles, we refer the interested reader to the work of Breugem [4,3]. In [3, Chapter 4], he explains how to obtain the porosity and permeability profiles of the variable-permeability model at the mesoscopic scale from a direct numerical simulation at the microscopic scale, using the volume averaging method and an appropriate filter. Following this approach, we performed a 2D microscopic simulation on the same flow geometry to obtain the porosity and the permeability profiles. This geometry is recalled in Fig. 1 (microscopic description). In the y-direction, the porous medium is made of seven cubes of size d_{p}. The distance between two cubes is also d_{p} and the size of the domain in the y-direction is fixed by taking $h = h_{\mathrm{b}} = 16d_{\mathrm{p}}$, where h_{b} is the height of the porous medium. In the horizontal direction, periodic boundary conditions are used. The results obtained for the porosity and the permeability profiles are given in Fig. 3. It is interesting to note that the permeability and the porosity do not vary over the same distance. The size of the heterogeneous transition region is about 3 d_{p} for the porosity and about 5 d_{p} for the permeability (see Fig. 3). It is therefore not possible to express the permeability as a function of the porosity in the transition region, as was proposed by Ochoa-Tapia and Whitaker [16] and Goyeau et al. [9].

It is worth noting that the porosity and permeability profiles can also be deduced from experimental data. Indeed, the porosity variations are easily deduced from photographs of the transition region [20,8]. To obtain the permeability profile, one needs first to compute the variations of the second derivative of the longitudinal velocity

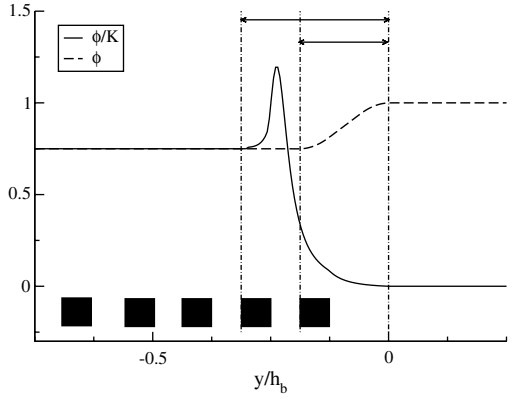

Fig. 3. Example of porosity and permeability profiles obtained by filtering microscopic results obtained from microscopic 2D simulations.

(see Eq. (4)). Saleh et al. [20] show that it is possible to obtain this information (see their Figs. 15 and 16). Given the typical profile of the second derivative that they obtain (see their Fig. 14), non-monotonic permeability profiles would be deduced as in our numerical simulation.

3.3. First results

Once the porosity and permeability profiles are known, the velocity at the mesoscopic scale can be obtained by solving Eq. (4) numerically. The solution of the MAE macroscopic problem is obtained by solving Eqs. (9) and (10) analytically, using the jump conditions (11) and (17) and the definition of the excess quantities proposed previously (22). The analytical solution of this problem is given in Appendix A. The solution of the OS macroscopic problem is obtained by solving the same problem but using the second jump condition (18). The analytical solution of this second problem is given in Appendix B.

The mesoscopic solution and the MAE macroscopic solutions obtained using the porosity and permeability profiles of the previous section (see Fig. 3), when $h = h_b$, are plotted in Fig. 4a for three different values of y_M. This figure shows that the MAE macroscopic velocity is not correctly predicted in the free fluid channel, and this, whatever the choice of y_M. Moreover, we observe that the choice of y_M has hardly any influence on the MAE velocity profile in the free fluid region. It seems that the linear dependence of the excess quantities on y_M allows to have a free fluid velocity in the channel almost independent of the choice of y_M. In Appendix C, it is proven that this is indeed the case by rewritting the analytical solution of the free macroscopic velocity in a new system of coordinates independent of the location of the discontinuous interface y_M. The two excess quantities *do* depend linearly on y_M. But this dependence does not influence the outer profiles, since due to this dependence, the MAE macroscopic free fluid velocity remains almost independent of y_M.

In Fig. 4b, the mesoscopic solution is compared to the solutions obtained by solving the OS macroscopic problem for three different values of y_M. This figure shows that the OS macroscopic solution is not at all correctly predicted in the free fluid channel. Furthermore, the OS macroscopic solutions are very different from the MAE macroscopic solutions. In particular, for the OS macroscopic problem, the choice of y_M has a very large influence on the velocity profile in the free fluid region.

These first results suggest that something is missing in the matched asymptotic expansion analysis, since the MAE macroscopic velocity is not correctly predicted in the free fluid channel. This problem will be tackled in the following section. These results also show that substituting $\langle u \rangle^{(0)}$ by $\langle u \rangle$ in the jump condition to simplify the resolution of the macroscopic problem has important consequences and therefore should not be used.

4. Matched asymptotic expansions under conservation constraint

4.1. Excess quantities and surface-excess forces

At the mesoscopic scale, the flow in the entire domain is described by Eq. (4). This equation expresses the balance between three forces: the friction force (μ (ϕ/K) u), the pressure force ϕ (dp/dx) and the viscous force μ (d^2u/dy^2). In this model, the porosity and permeability are varying only in the interfacial transition zone; they are constant in the two homogeneous regions. At the macroscopic scale, the flow is governed by Eqs. (9) and (10) where the porosity and permeability are constant in each homogeneous region. By construction, at this scale, the friction force and the pressure force are not properly described in the interfacial transition zone since the porosity and the permeability are constant. In the study of interfacial phenomena, the difference of any physical quantity between its mesoscopic and its macroscopic values in the interfacial transition zone can be expressed through excess quantities [7]. For instance, the excess quantity associated to the friction force is given by:

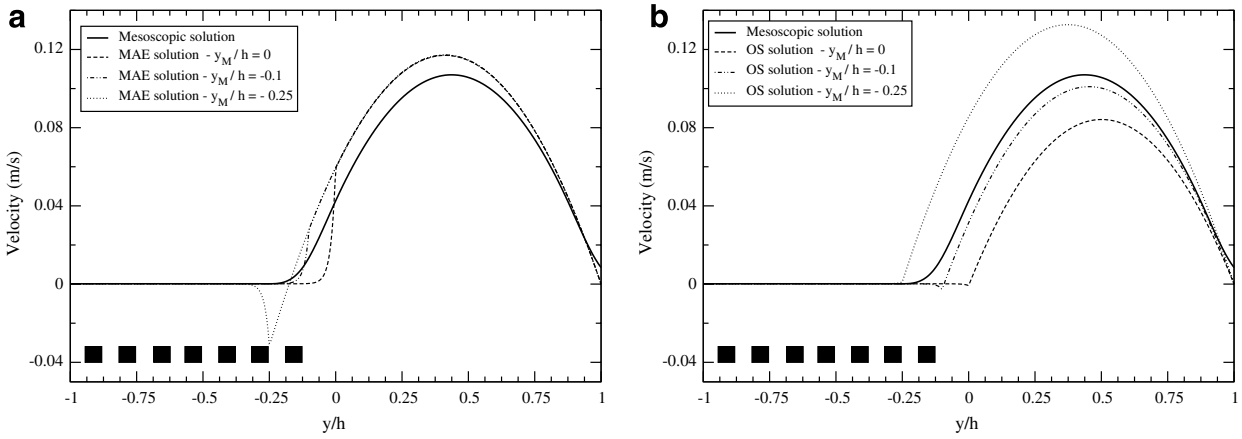

Fig. 4. Mesoscopic, MAE and OS macroscopic velocity results obtained using the original definition (22) of the excess quantities. (a) Comparison of the mesoscopic and MAE macroscopic solutions. (b) Comparison of the mesoscopic and OS macroscopic solutions.

$$\left(\mu\frac{\phi}{K}u\right)^{\mathrm{exM}} = \mu\int_{-\infty}^{y_{\mathrm{M}}}\left(\frac{\phi}{K}u_{\mathrm{c}} - \frac{\phi_{\mathrm{p}}}{K_{\mathrm{p}}}u_{\mathrm{d}}\right) + \mu\int_{y_{\mathrm{M}}}^{h}\left(\frac{\phi}{K}u_{\mathrm{c}}\right) \tag{23}$$

where u_{c} is the velocity solution of the mesoscopic problem and u_{d} is the velocity solution of a given macroscopic problem (either the MAE or the OS macroscopic problem). The excess quantity $(\mu\,(\phi/K)\,u)^{\mathrm{exM}}$ represents *exactly* the amount of the force that is not seen by the macroscopic model in the interfacial transition zone compared to the mesoscopic model. However, this amount of force has to be taken into account to give an accurate description of the problem at the macroscopic scale. This is done by assigning this surface-excess force to the macroscale surface *via* a stress jump condition. The main difficulty is to express this excess quantity using only macroscopic parameters in order to close the macroscopic problem. In this framework, the results obtained in [5] using the matched asymptotic expansion analysis can be viewed in a new way. The matched asymptotic expansion allows to obtain a linearized form of the friction surface-excess force that depends only on macroscopic quantities:

$$\left(\mu\frac{\phi}{K}u\right)^{\mathrm{exM}} \simeq \mu\left(\frac{\phi}{K}\right)^{\mathrm{exM}}\langle u\rangle^{(0)}\big|_{y_{\mathrm{M}}} \tag{24}$$

However, this expression is only an approximation at first order.

Let us now consider the two other forces, *i.e.* the pressure and viscous forces. For the pressure force, the result obtained in [5] is not an approximation but is exact since the pressure gradient is constant:

$$\left(\phi\frac{\mathrm{d}p}{\mathrm{d}x}\right)^{\mathrm{exM}} = (\phi)^{\mathrm{exM}}\frac{\mathrm{d}p}{\mathrm{d}x} \tag{25}$$

The pressure surface-excess force is therefore exactly conserved in this expression.

For the viscous surface-excess force, the excess quantity depends only on macroscopic quantities or on mesoscopic quantities located in the homogeneous free fluid region:

$$\left(\mu\frac{\mathrm{d}^2u}{\mathrm{d}y^2}\right)^{\mathrm{exM}} = \mu\left(\frac{\mathrm{d}u_{\mathrm{c}}}{\mathrm{d}y}\bigg|_{\mathrm{h}} - \frac{\mathrm{d}u_{\mathrm{d}}}{\mathrm{d}y}\bigg|_{\mathrm{h}}\right) - \mu\left(\frac{\mathrm{d}u_{\mathrm{d}}}{\mathrm{d}y}\bigg|_{y_{\mathrm{M}}^{+}} - \frac{\mathrm{d}u_{\mathrm{d}}}{\mathrm{d}y}\bigg|_{y_{\mathrm{M}}^{-}}\right) \tag{26}$$

Since the macroscopic model is supposed to be such that the mesoscopic and macroscopic solutions are equal in the two homogeneous regions, the first term in the right hand side of Eq. (26) is zero. The second term in the right hand side of Eq. (26) is exactly the stress jump that is assigned to the macroscopic surface. The stress jump condition (17) is simply recovered in this framework, by adding Eqs. (24)–(26).

These developments show that the only approximation of the surface-excess forces is due to the friction force, as shown by Eq. (24). The effects of this approximation are too important to be neglected since, using this expression, the MAE macroscopic velocity is not correctly predicted (see Section 3.3). Thus, the question is the following: is it possible to obtain a new linearized expression for the excess quantity associated to the friction surface-excess force such that this surface-excess force is *exactly* conserved? To answer this question, the analytical study made using the matched asymptotic expansions will be revisited under the constraint of conservation of the friction surface-excess force.

4.2. Introduction of the conservation constraint

In the matched asymptotic expansion study carried out in [5], as $\epsilon \to 0$, the porosity and permeability profiles are modified. Indeed, the porosity and permeability profiles depend on the inverse of δ (see Eqs. (38) and (39) for example). Since $\epsilon = \delta/h$, as $\epsilon \to 0$, h being kept constant, the profiles become stiffer to give, at the limit, profiles that are discontinuous at y_{M} (the matched asymptotic expansion is carried out around the position $y = y_{\mathrm{M}}$). As $\epsilon \to 0$, if the profile of a physical quantity ψ becomes stiffer around its center of gravity y_{ψ}, the integral of the physical profile of ψ minus its limit discontinuous profile, is zero: the ψ quantity is exactly conserved in the up-scaling. Now, if the discontinuous interface is located at a position y_{M} different from y_{ψ}, the excess quantity ψ^{exM} (Eq. (22)) accounts exactly for the gap between y_{ψ} and y_{M} (see Fig. 2c).

The pressure force is related to the porosity profile. However, when the porosity profile tends to a Heaviside function as $\epsilon \to 0$, since the pressure gradient does not depend on the porosity, the conservation of the porosity through $(\phi)^{\mathrm{exM}}$ ensures the conservation of the pressure force. For the friction force, it is different. This force is related to the profile of ϕ/K but also to the velocity. But now, the velocity depends directly on the profile of ϕ/K. Hence, as the profile of ϕ/K becomes stiffer, the velocity is modified and the friction force might not be conserved as $\epsilon \to 0$, if the constraint is not enforced. If the center of gravity of the profile of ϕ/K was the same as the center of gravity of the friction force, the friction force would be conserved in the up-scaling performed previously. Unfortunately, there is no reason that this is indeed the case.

To be more precise, the evaluation of the friction surface-excess force in the matched asymptotic expansion analysis depends only on the profile of ϕ/K and on the zeroth order velocity in the *inner region* (see [5]). From the matched asymptotic expansion analysis [5], we know that the zeroth order velocity is constant in the *inner region*. This result allows to obtain the linearized form of the friction surface-excess force (24). The positive point about this result is that the obtained linear dependence on y_{M} of the closure expression for the friction surface-excess force allows to have a macroscopic free fluid velocity in the channel almost independent of the choice of y_{M} (see Section 3.3). The negative point is that the friction surface-excess

force is not conserved because the center of gravity of the profile of ϕ/K is not in general the same as the center of gravity of the friction force. Therefore, we suggest to introduce the following new excess quantity associated to the friction surface-excess force

$$\left(\mu\frac{\phi}{K}u\right)^{\mathrm{exM}} = \mu\left(\frac{\phi}{K}\right)^{ex\Delta}\langle u\rangle^{(0)}|_{y_\mathrm{M}} \tag{27}$$

with

$$\left(\frac{\phi}{K}\right)^{ex\Delta} = \left(y_{\phi/K}+\Delta y - y_\mathrm{M}\right)\left(\frac{\phi_\mathrm{p}}{K_\mathrm{p}}\right) \tag{28}$$

where $(y_{\phi/K}+\Delta y)$ is the center of gravity of the friction force. Thus, the friction surface-excess force is conserved in the up-scaling analysis and the linear dependence on y_M of the closure expression for the friction surface-excess force is not modified. Since the size of the transition zone is δ, we expect Δy to be of the order of δ. At this point Δy is unknown and its determination is examined in the following section.

4.3. Determination of Δy

By construction Δy is such that the friction surface-excess force is exactly conserved in the matched asymptotic expansion analysis. Since the viscosity is constant, it comes from Eqs. (23) and (27):

$$\int_{-\infty}^{y_\mathrm{M}}\left(\frac{\phi}{K}u_\mathrm{c}-\frac{\phi_\mathrm{p}}{K_\mathrm{p}}u_\mathrm{A}\right)+\int_{y_\mathrm{M}}^{h}\left(\frac{\phi}{K}u_\mathrm{c}\right)=\left(\frac{\phi}{K}\right)^{ex\Delta}\langle u\rangle^{(0)}|_{y_\mathrm{M}} \tag{29}$$

The determination of Δy requires to solve Eq. (29). The resolution of this equation requires the specification of u_c, that is unfortunately unknown. This difficulty is overcome by following an indirect approach.

The mesoscopic solution verifies Eq. (4). This equation is integrated between $y=-\infty$ and h:

$$\left.\frac{\mathrm{d}u_\mathrm{c}}{\mathrm{d}y}\right|_h = \int_{-\infty}^{h}\left(\frac{\phi}{K}u_\mathrm{c}+\frac{\phi}{\mu}\frac{\mathrm{d}p}{\mathrm{d}x}\right) \tag{30}$$

The MAE macroscopic solution verifies Eqs. (9) and (10), with the jump conditions (11) and (17) at the interface. Eq. (10) is integrated between $y=-\infty$ and $y=y_\mathrm{M}$ and Eq. (9) between $y=y_\mathrm{M}$ and $y=h$:

$$\begin{aligned}\left.\frac{\mathrm{d}u_\mathrm{A}}{\mathrm{d}y}\right|_h &= \int_{-\infty}^{y_\mathrm{M}}\left(\frac{\phi_\mathrm{p}}{K_\mathrm{p}}u_\mathrm{A}+\frac{\phi_\mathrm{p}}{\mu}\frac{\mathrm{d}p}{\mathrm{d}x}\right)+\int_{y_\mathrm{M}}^{h}\frac{1}{\mu}\frac{\mathrm{d}p}{\mathrm{d}x}\\ &\quad+\left(\frac{\phi}{K}\right)^{ex\Delta}\langle u\rangle^{(0)}|_{y_\mathrm{M}}+(\phi)^{\mathrm{exM}}\frac{1}{\mu}\frac{\mathrm{d}p}{\mathrm{d}x}\end{aligned} \tag{31}$$

Subtracting Eqs. (30) and (31) shows that, when the pressure and friction surface-excess forces are *exactly* conserved, one has:

$$\left.\frac{\mathrm{d}u_\mathrm{c}}{\mathrm{d}y}\right|_h = \left.\frac{\mathrm{d}u_\mathrm{A}}{\mathrm{d}y}\right|_h \tag{32}$$

And inversely, when the relation (32) is verified, since the pressure surface-excess force is conserved (Eq. (25)), we can deduce that the friction surface-excess force is also conserved. Since the mesoscopic and macroscopic velocity profiles are parabolic in the homogeneous free fluid region and both vanish at $y=h$, when Eq. (32) is verified the mesoscopic and macroscopic velocity parabolic profiles are equal. This shows that the *exact* conservation of the friction surface-excess force is the key feature that has to be imposed to recover the correct velocity profile in the free fluid region when the system is described at the macroscopic scale.

4.3.1. Velocity in the free fluid region at the mesoscopic scale

In the homogeneous free fluid region ($\phi=1,\quad 1/K=0$), the solution of the mesoscopic problem u_c verifies

$$\mu\frac{\mathrm{d}^2u_\mathrm{c}}{\mathrm{d}y^2}=\frac{\mathrm{d}p}{\mathrm{d}x} \tag{33}$$

with a no slip boundary condition at the upper wall. The velocity profile is then extended in the heterogeneous transition region. The location where this extended velocity profile vanishes is called the *equivalent impermeable wall* and is noted y_imp. Indeed, if the porous medium is replaced by an impermeable wall, this impermeable wall would be located at y_imp to conserve the parabolic profile of the velocity in the free fluid channel. Therefore, y_imp characterizes the velocity in the free fluid channel at the mesoscopic scale.

4.3.2. Velocity in the free fluid region at the macroscopic scale for the MAE problem

We now want to characterize the velocity in the free fluid channel at the macroscopic scale. The analytical expression of the solution of the MAE problem in the free fluid channel is given by Eq. (44) in Appendix A, where $(\phi/K)^{\mathrm{exM}}$ has to be replaced by $(\phi/K)^{ex\Delta}$ in Eq. (47). The extended parabolic profile of the solution in the free fluid region vanishes at:

$$y = y_\mathrm{M}+\sigma\sqrt{K_\mathrm{p}}\left(\frac{2(C_2^{(0)}+\epsilon C_2^{(1)})}{\sigma^2}-1\right) \tag{34}$$

(see Appendix A for the definitions of σ, $C_2^{(0)}$ and $C_2^{(1)}$). To simplify this expression the discontinuous interface is located at $y_\mathrm{M}=(y_{\phi/K}+\Delta y)$. Thus, the excess quantity associated to the friction force is zero. It comes:

$$y=(y_{\phi/K}+\Delta y)-\frac{2\sqrt{\phi_\mathrm{p}}\sqrt{K_\mathrm{p}}+2(\phi)^{\mathrm{exM}}+\sigma\sqrt{K_\mathrm{p}}}{1+\sqrt{\phi_\mathrm{p}}\sigma} \tag{35}$$

Here, the value of $(\phi)^{\mathrm{exM}}$ is given by Eq. (22), with $y_\mathrm{M}=(y_{\phi/K}+\Delta y)$. Since $\sqrt{K_\mathrm{p}}/(h-y_\mathrm{M})=1/\sigma$ is small compared to one and assuming that (ϕ^{exM}) is always small compared to h, one gets:

$$y\sim(y_{\phi/K}+\Delta y)-\sqrt{\frac{K_\mathrm{p}}{\phi_\mathrm{p}}} \tag{36}$$

Therefore, Eq. (36) characterizes indirectly the velocity in the free fluid channel at the macroscopic scale.

If the following relation is verified:

$$y_{\text{imp}} = y_{\phi/K} + \Delta y - \sqrt{\frac{K_{\text{p}}}{\phi_{\text{p}}}} \tag{37}$$

the mesoscopic and the MAE macroscopic extended parabolic profiles of the velocity are equal and therefore Eq. (32) is verified. Since we have shown previously the equivalence between Eq. (32) and the conservation of the friction surface-excess force, this conservation is indirectly obtained by imposing the condition (37). Therefore, the conservation of the friction surface-excess force is indirectly obtained. This reasoning, based on the introduction of a new excess quantity associated to the friction surface-excess force is valid only if the value of $(\phi/K)^{\text{ex}\Delta}$ does not depend on the height of the free channel h. If this were not the case, the generality of the approach would be lost as well as the interfacial intrinsic character of Δy. As we will see in Section 5, Δy barely depends on h, which confirms the above interpretation.

5. Comparisons to numerical results

5.1. Description of the 1D problem

To quantify the effect of a given porous medium, Beavers and Joseph [1] compared the mass flow rate in the free fluid channel obtained with a permeable lower wall to the one that would be obtained with an impermeable wall for different heights of the free fluid channel. Here, we numerically reproduce these experiments for four different materials by considering different heights of the free channel: $h = h_{\text{b}}$, 1.25 h_{b}, 1.5 h_{b}, 1.75 h_{b} and 2 h_{b}.

The properties of the homogeneous porous medium are fixed: $h_{\text{b}} = 16\ d_{\text{p}}$ and $\phi_{\text{p}} = 0.75$ as in the DNS of Section 3.2, and $K_{\text{p}} = d_{\text{p}}^2/18$, which is a good estimate of the homogeneous permeability obtained with the 2D DNS. Then the value of h_{b} is fixed to 1, which gives $d_{\text{p}} = 0.0625$ and $K_{\text{p}} = 2.17 \times 10^{-4}\ \text{m}^2$. For the size of the heterogeneous transition region, the ratio δ/d_{p} is fixed to 3. In all the study, the pressure gradient is kept constant. The ratio $\nabla p/\mu$ is fixed to -1.

At the mesoscopic scale, a material is characterized by its porosity and permeability profiles in the heterogeneous transition zone. For the first three materials, the same porosity profile is used:

$$\phi(y) = \frac{1-\phi_{\text{p}}}{2}\tanh\left(\frac{2y}{\delta}\right) + \frac{1+\phi_{\text{p}}}{2} \tag{38}$$

For the permeability, different profiles are tested. For the first material, we consider a hyperbolic tangent profile:

$$\left(\frac{1}{K}\right)(y) = \frac{1}{K_{\text{p}}}\left(\frac{-1}{2}\tanh\left(\frac{2y}{\delta}\right) + \frac{1}{2}\right) \tag{39}$$

Then, more complex profiles are used that are more representative of the profiles obtained from experiments [20] or filtered DNS [3,4] (see Fig. 3). For the second material, the chosen permeability profile is:

$$\left(\frac{1}{K}\right)(y) = \frac{1}{K_{\text{p}}}\left[\frac{-1}{2}\tanh\left(\frac{2y}{\delta}\right) + \frac{1}{2} + 1 - \left(\tanh\left(\frac{2y}{\delta}\right)\right)^2\right] \tag{40}$$

For the third material, the permeability profile is similar but shifted:

$$\left(\frac{1}{K}\right)(y) = \frac{1}{K_{\text{p}}}\left[\frac{-1}{2}\tanh\left(\frac{2(y+1.5\delta)}{\delta}\right) + \frac{1}{2} + 1 - \left(\tanh\left(\frac{2(y+1.5\delta)}{\delta}\right)\right)^2\right] \tag{41}$$

Then for the fourth material, a more complex porosity profile is studied, that is supposed to characterize mass storage in the transition region:

$$\phi(y) = \frac{1-\phi_{\text{p}}}{2}\tanh\left(\frac{2y}{\delta}\right) + \frac{1+\phi_{\text{p}}}{2} - 0.4\left[1 - \left(\tanh\left(\frac{2y}{\delta}\right)\right)^2\right] \tag{42}$$

and the profile of ϕ/K is supposed to be given by a simple hyperbolic tangent function:

$$\left(\frac{\phi}{K}\right)(y) = \frac{\phi_{\text{p}}}{K_{\text{p}}}\left(\frac{-1}{2}\tanh\left(\frac{2y}{\delta}\right) + \frac{1}{2}\right) \tag{43}$$

These different profiles are represented in Fig. 5. The values of y_{ϕ} and $y_{\phi/K}$ obtained for the four materials are provided in Table 2.

The velocity profiles at the mesoscopic scale are obtained by solving Eq. (4) numerically, with no slip boundary conditions at $y = h$ and $y = h_{\text{b}}$.

In Section 4.3, we underlined that our analysis is valid only if the value of Δy does not depend on h. Thus, this hypothesis is checked first. For each material and each free channel height, the value of y_{imp} is obtained by extending the parabolic profile of the mesoscopic solution inside the porous region. Then, Δy is computed using Eq. (37). The results for Δy are presented in Table 1. Δy is almost independent of h, which substantiates our analysis. The mean value of Δy obtained for each material is also presented. This also shows that only one simulation at the mesoscopic scale with an arbitrary h is sufficient to compute y_{imp} and then to determine Δy using Eq. (37).

5.2. Velocity results

In Fig. 6, the mesoscopic velocity profiles u_{c} obtained by solving Eq. (4) numerically are compared to the MAE macroscopic profiles computed analytically using the new

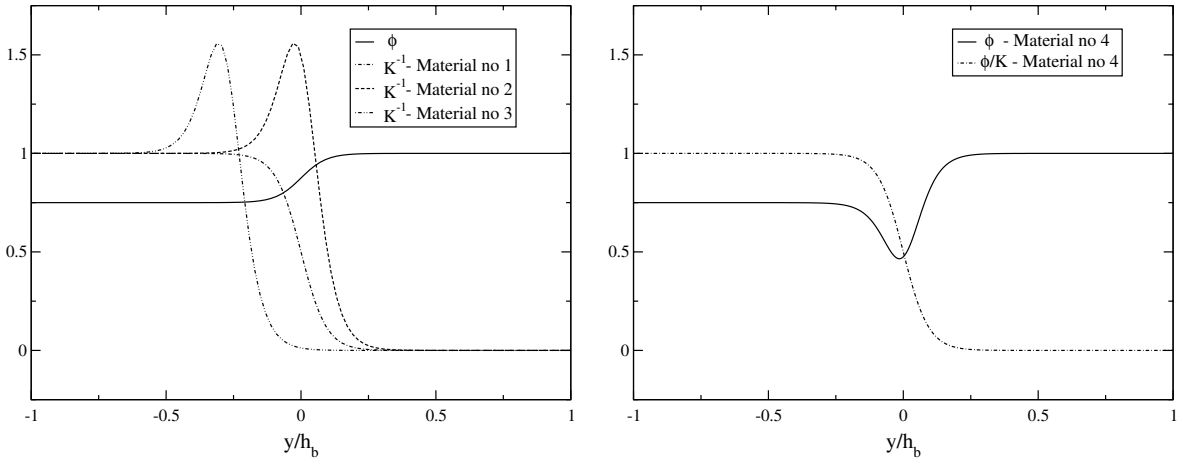

Fig. 5. Non-dimensional porosity and permeability profiles for the four materials considered in the study.

Table 1
Result obtained for Δy as a function of h for the different materials

h/h_b	1	1.25	1.5	1.75	2	Mean Δy
Material no. 1	0.1534	0.1554	0.1554	0.1574	0.1574	0.1558
Material no. 2	0.0107	0.0135	0.0153	0.0127	0.0157	0.0136
Material no. 3	0.0565	0.0575	0.0575	0.0581	0.0565	0.0572
Material no. 4	0.1570	0.1590	0.1600	0.1610	0.1620	0.1600

definition of the friction excess quantity $(\phi/K)^{ex\Delta}$. The macroscopic profiles are computed with the discontinuous interface located at y_M such that the quantity $(y_M - y_{\phi/K} - \Delta y)$ is positive. When this constraint is not satisfied, the result is not physical since negative slip velocities are obtained at the interface. However, provided that this constraint is satisfied, the choice of y_M in the transition region is arbitrary since it was proven in Section 3.3 that it has no consequence on the macroscopic velocity profile in the free fluid region. Thus, we choose to locate the discontinuous interface at $y_M = 0.2$ for the first material, $y_M = 0.25$ for the second, $y_M = 0$ for the third and $y_M = 0.2$ for the fourth material. The excess quantities computed with these values of y_M are presented in Table 2. One can notice that the constraint $(y_M - y_{\phi/K} - \Delta y) > 0$ implies that $(\phi/K)^{ex\Delta}$ is negative. Fig. 6 shows that for the four materials, the MAE macroscopic velocity in the free fluid region is very well predicted. This supports the discussion on the excess quantity and the introduction of the conservation constraint in the matched asymptotic expansions analysis.

In Fig. 7, a zoom of the solution obtained for the third material in the transition region is presented. The velocity is not correctly predicted by the macroscopic model compared to the mesoscopic one in the transition region. This is not surprising since by construction the macroscopic model is appropriate to describe the problem only in the two homogeneous regions, where the porosity and permeability are constant. This difference between the mesoscopic and the macroscopic results has also been observed and highlighted by Goyeau et al. [9] (see their Fig. 9).

5.3. A priori estimation of Δy

With the reasoning of Section 4.3, one still has to determine the location of the equivalent impermeable wall y_{imp} to deduce the value of Δy. In this study, it is determined numerically from the resolution of the mesoscopic problem for a particular but arbitrary value of h. The difficulty to determine Δy *a priori* is that in Eq. (29) Δy still depends on u_c, that is of course unknown. However, since u_c and u_A differ only in a small region, if u_c is replaced by u_A in Eq. (29) we can expect to obtain a first estimate of Δy. To simplify the calculation, the discontinuous interface is located at $(y_{\phi/K} + \Delta y)$. The macroscopic solution u_A is known analytically and is given in Appendix A, where $(\phi/K)^{exM}$ has to be replaced by $(\phi/K)^{ex\Delta}$ in Eq. (47). The results obtained using this approach are presented in Table 3. The trend is good even though we seem to always underestimate the value of Δy by a constant value of approximately 0,05. But, this estimate is not accurate enough, since the error can be of the same order as the value, which implies that the results obtained with this approximation are neither worse nor better than those obtained with $\Delta y = 0$ (matched asymptotic expansion without constraint). So far, we are not able to predict the value of Δy prior to any simulation.

5.4. Summary

Before discussing the results that have been obtained, we summarize what has to be done to obtain the solution of the MAE macroscopic problem starting from given porosity and permeability profiles in the heterogenous transition region at the mesoscopic scale. The values of y_ϕ and $y_{\phi/K}$ are deduced from the porosity and permeability profiles using Eq. (21). One simulation at the mesoscopic scale has to be run for an arbitrary value of the free channel height to determine the location of the equivalent impermeable wall y_{imp}. This is done by extending the parabolic pro-

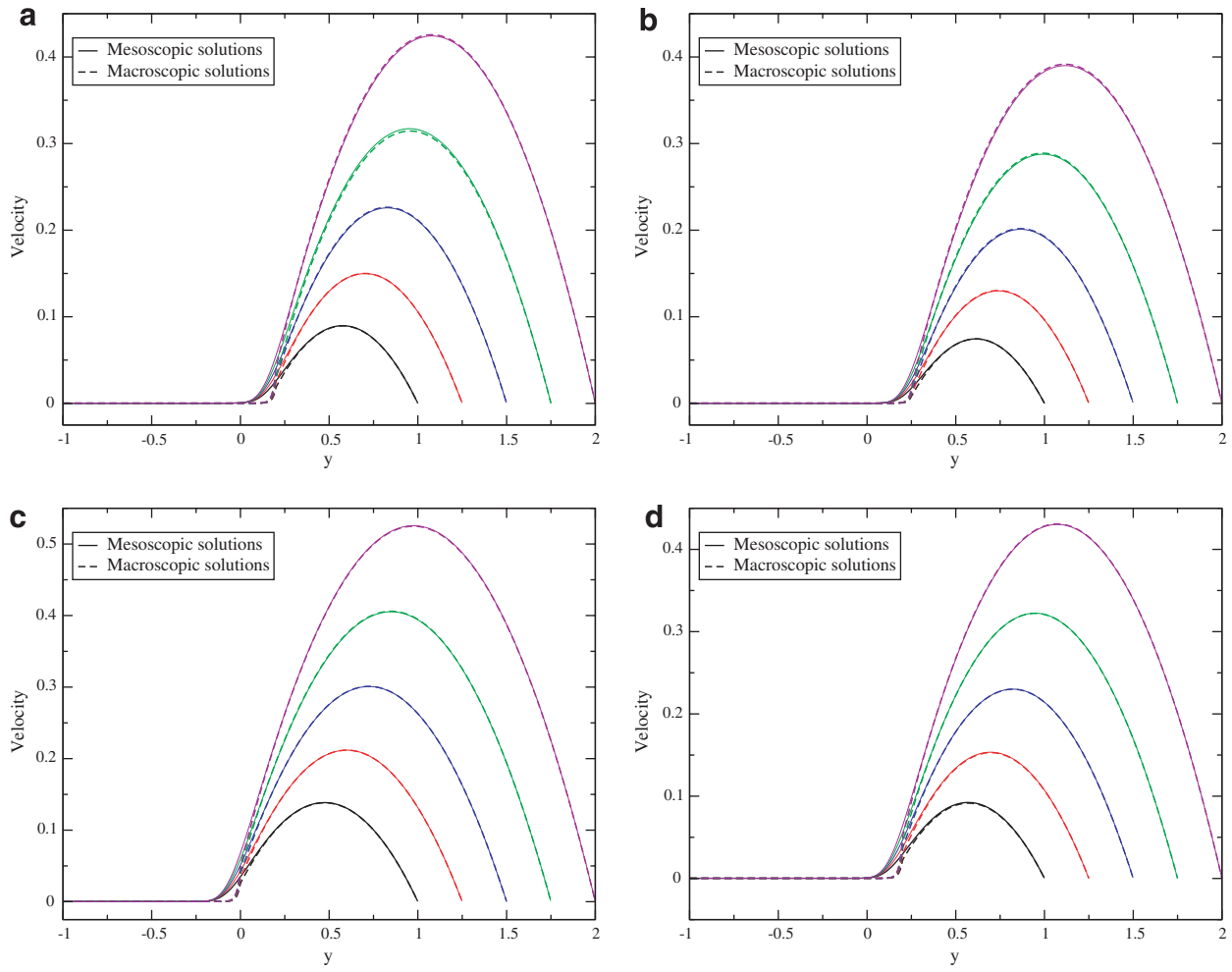

Fig. 6. Comparison of the mesoscopic and macroscopic solutions obtained using the new definition (28) of the excess quantity associated to the friction force. (a) Material no. 1: $y_M = 0.2$, (b) Material no. 2: $y_M = 0.25$, (c) Material no. 3: $y_M = 0$, (d) Material no. 4: $y_M = 0.2$.

Table 2
Results from the numerical study at the mesoscopic scale

Material	y_ϕ	$y_{\phi/K}$	y_{imp}	Δy	y_M	$(\phi)^{exM}$	$(\phi/K)^{exM}$	$(\phi/K)^{ex\Delta}$
No. 1	0	0.0156	0.1544	0.1558	0.2	0.05	−637	−99
No. 2	0	0.2343	0.2310	0.0136	0.25	0.0625	−54	−7
No. 3	0	−0.0925	−0.0523	0.0572	0	0	−320	−122
No. 4	0.3	0	0.1428	0.16	0.2	−0.025	−691	−139

file of the mesoscopic velocity inside the porous region. Then, the value of Δy can be deduced from these results using Eq. (37). At this point, to compute the values of the two excess quantities $(\phi)^{exM}$ and $(\phi/K)^{ex\Delta}$, using Eq. (22) for the pressure force and Eq. (28) for the friction force, only the location of the discontinuous interface y_M is missing. As seen in Section 3.3, this choice has no consequence on the macroscopic velocity profile as long as y_M belongs to the transition region and is such that $(y_M - y_{\phi/K} - \Delta y)$ remains positive. For a given position y_M, one can obtain the values of the two excess quantities and solve the MAE macroscopic problem using the stress jump condition (17) at y_M.

6. Discussion

6.1. Intrinsic interfacial properties

The dependence of the excess quantities on the location of the surface of discontinuity y_M is not compatible with the idea of *intrinsic* interfacial properties. Therefore, we cannot state that these excess quantities are intrinsic interfacial properties. However, the structure of the transition region is shown to be characterized by three structural parameters that are true intrinsic interfacial properties: $y_{\phi/K}$, y_ϕ and Δy. The center of gravity of the profiles of ϕ and ϕ/K (y_ϕ and $y_{\phi/K}$) are given by the permeability and

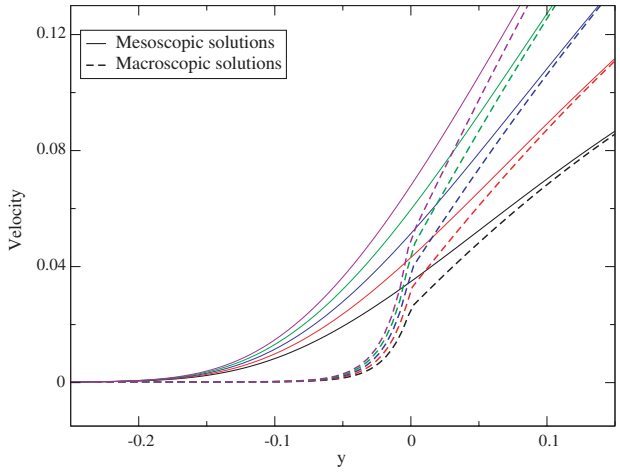

Fig. 7. Zoom on the transition region – third material.

Table 3
Comparison of the actual values and estimated values of Δy

	Estimation	Δy
Material no. 1	0.1074	0.1558
Material no. 2	−0.0323	0.0136
Material no. 3	0.0077	0.0572
Material no. 4	0.102	0.16

porosity profiles (Eq. (21)). The determination of Δy is much more complex and relies on the constraint of conservation of the friction surface-excess force. We have shown how to obtain its value for given porosity and permeability profiles and it is verified that its value is indeed independent of h, the height of the free fluid channel, which confirms its intrinsic character.

6.2. Porous boundary layer

The use of the Darcy-Brinkman equation has also to be addressed. In general, the Darcy-Brinkman model is introduced to be able to describe the boundary layer region within the porous region. The choice of the Darcy-Brinkman equation combined with a variable permeability and porosity model, can be justified at the mesoscopic scale of description: filtered DNS data are very well represented by this model [3]. However, at the macroscopic scale (constant porosity and permeability) one has to be careful with the interpretation of the results obtained with the Darcy-Brinkman equation. Indeed, is the macroscopic model able to correctly describe the porous boundary layer?

The porous boundary layer is defined as the layer between the interface and the location in the porous region where the velocity approaches its equilibrium value U_∞. Since this definition is related to the interface, it is a notion associated to the macroscopic level of description. However, at the macroscopic scale, the velocity decays exponentially in the porous region (see Eq. (45)). Therefore, we know that the size of the boundary layer obtained with the macroscopic model is of order $\sqrt{K_p/\phi_p}$. Since $\sqrt{K_p} \sim d_p \sim \delta$, the thickness of the transition region and of the boundary layer are of the same order. Thus, the porous boundary layer region is inseparable from the interfacial transition region. However, by construction, the macroscopic model is not appropriate to describe the problem in the heterogeneous transition region. Therefore, the macroscopic model is not able to correctly describe the porous boundary layer. This is clearly visible in Fig. 7, where the macroscopic model underestimates the velocity in the transition region and therefore underestimates the size of the porous boundary layer. This study shows that the size of the boundary layer thickness cannot be determined from a model with two homogeneous regions separated by a discontinuous interface.

7. Conclusion

The objective of this study was to show that it is possible to provide an explicit relation between the values of the jump parameters of the stress jump condition that one should impose at a free-fluid/porous interface and the structure of the transition region. In [5], an explicit relation is proposed between the two jump parameters and the porosity and permeability variations in the transition zone through excess quantities. For given porosity and permeability profiles, the computation of the excess quantities should have been direct. However, using the relation obtained in [5], the macroscopic velocity in the free fluid region is not correctly predicted. This is the consequence of the non-*exact* conservation of the friction surface-excess force in the matched asymptotic expansions analysis. Therefore, this analysis has been revisited to impose the constraint of conservation of the friction surface-excess force and the excess quantity associated to the friction force has been redefined. The important result is that, using this new definition of the excess quantity associated to the friction force, the values of the two jump parameters are directly related to the structure of the transition region through three structural quantities: $y_{\phi/K}$, y_ϕ and Δy (Eqs. (22) and (28)) without any adjustable parameter. Furthermore, this analysis makes explicit the linear dependence between the jump parameters and the location of the discontinuous interface, a dependence that has been observed in previous studies [18,10,19,4]. It is proven that, as a consequence of this dependence, the velocity in the free channel remains independent of the arbitrary choice of the location of the discontinuous interface. Therefore, this analysis proves that there is no best choice for the location of the discontinuous interface inside the transition region, as long as $(y_M - y_{\phi/K} - \Delta y)$ remains positive. These results are illustrated by numerically studying 1D problems similar to the Beavers and Joseph experiments. Very good agreement is obtained between the mesoscopic and the MAE macroscopic solutions.

An important advantage of this study is also the introduction of the three scales of description: microscopic, mes-

oscopic and macroscopic. This introduction clarifies the hypotheses attached to each scale of description. For example, the interface is a macroscopic notion, whereas it is shown that the size of the porous boundary layer is a mesoscopic notion. Furthermore, the two up-scalings from one scale of description to another (microscopic → mesoscopic and mesoscopic → macroscopic) have been made explicit, suggesting a methodology to derive boundary conditions for other transport phenomena.

Acknowledgement

The authors thank Pierre Ruyer for very helpful discussions.

Appendix A. Analytical solution of the MAE macroscopic problem

The solution of the MAE macroscopic problem is obtained by solving Eqs. (9) and (10) analytically, using the jump conditions (11) and (17). This analytical solution is given in [5] and is recalled here for completeness concern and also to give the more general form of the result when the discontinuous interface is located at y_M and not at $y = 0$:

$$u_A(y) = U_\infty \left[\frac{-\sigma^2}{2} \left(\frac{(y-y_M)^2}{(h-y_M)^2} - 1 \right) + \left(C_2^{(0)} + \epsilon C_2^{(1)} \right) \left(\frac{y-y_M}{h-y_M} - 1 \right) \right], \quad y_M \leqslant y \leqslant h \tag{44}$$

$$u_A(y) = U_\infty \left(1 + C_1^{(0)} + \epsilon C_1^{(1)} \right) \exp\left(\sqrt{\frac{\phi_p}{K_p}} (y - y_M) \right), \quad y \leqslant y_M \tag{45}$$

with

$$\sigma = \frac{h - y_M}{\sqrt{K_p}}, \quad C_1^{(0)} = \frac{\sigma^2 - 2}{2(1 + \sigma\sqrt{\phi_p})},$$
$$C_2^{(0)} = \sigma \sqrt{\phi_p} C_1^{(0)} \tag{46}$$

and

$$\epsilon C_2^{(1)} = \frac{\sigma}{\sqrt{K_p}(1 + \sigma\sqrt{\phi_p})} \left((1 + C_1^{(0)}) K_p \left(\frac{\phi}{K} \right)^{\text{exM}} - (\phi)^{\text{exM}} \right) = -C_1^{(1)} \tag{47}$$

This result is obtained from [5] by a simple change of variable.

Appendix B. Analytical solution of the OS macroscopic problem

The solution of the OS macroscopic problem is obtained by solving Eqs. (9) and (10) analytically, using the jump conditions (11) and (18). Using only the velocity continuity at the interface, the solution in the free fluid and porous region is given by:

$$u_{OS}(y) = \frac{1}{2\mu} \frac{dp}{dx} (y - h)(y - y_M) + u_B \frac{h - y}{h - y_M}, \quad y_M \leqslant y \leqslant h \tag{48}$$

$$u_{OS}(y) = (u_B - U_\infty) \exp\left(\sqrt{\frac{\phi_p}{K_p}} (y - y_M) \right) + U_\infty, \quad y \leqslant y_M \tag{49}$$

where $u_B = u_{OS}(y_M)$ is the slip velocity and the Darcy velocity U_∞ is expressed as follows:

$$U_\infty = -\frac{K_p}{\mu} \frac{dp}{dx} \tag{50}$$

The solution is still parameterized by u_B. The slip velocity is determined using the stress jump condition (18) at y_M:

$$u_B = \frac{U_\infty (h - y_M)}{2\sqrt{K_p}} \left(\frac{1 + 2 \frac{(\phi)^{\text{exM}} + \sqrt{\phi_p K_p}}{h - y_M}}{\sqrt{\phi_p} + \sqrt{K_p} \left(\frac{\phi}{K} \right)^{\text{exM}} + \frac{\sqrt{K_p}}{h - y_M}} \right) \tag{51}$$

Appendix C. Location of the discontinuous interface

Here, we prove that the MAE macroscopic velocity in the free fluid region is independent of the location of the discontinuous interface y_M by rewriting the analytical solution of the free macroscopic velocity in a new system of coordinates independent of the location of the discontinuous interface y_M. The analytical macroscopic solution for the velocity is expressed in the system of coordinates y and the solution depends on the sign of $(y - y_M)$ (see Eqs. (44) and (45)). Since the choice of y_M is arbitrary in the transition region, the analytical solution seems to depend on the location of the discontinuous interface. A new system of coordinates Y is now introduced such that $Y = 0$ when $y = y_{\phi/K}$. The choice of this system is no longer arbitrary since the quantity $y_{\phi/K}$ is an intrinsic property of the surface of a given material. This change of variable implies:

$$Y = y - y_{\phi/K} \tag{52}$$

$$H = h - y_{\phi/K} \tag{53}$$

The objective is to show that the macroscopic velocity u_A in the free fluid region is independent of y_M. Since u_A in the free fluid region is a parabola and vanishes at the upper wall whatever the choice of y_M, it is sufficient to show that du_A/dY is independent of y_M. From Eq. (44), in the y system of coordinate it comes:

$$\frac{du_A}{dy} = U_\infty \left(\underbrace{-\frac{y - y_M}{K_p}}_{B1} + \underbrace{\frac{C_2^{(0)} + \epsilon C_2^{(1)}}{\sigma\sqrt{K_p}}}_{B2} \right) \tag{54}$$

For more clarity, we introduce:

$$\Sigma = \frac{H}{\sqrt{K_p}}, \quad x = \frac{y_{\phi/K} - y_M}{H}, \quad \gamma = \frac{y_\phi - y_{\phi/K}}{H} \tag{55}$$

It comes:

$$B_1 = \frac{-Y}{K_p} - \frac{\Sigma}{\sqrt{K_p}}x \tag{56}$$

Using relations (22), (28), (52) and (55), the first order Taylor expansion in x of B_2 is:

$$B_2 = \frac{\sqrt{\phi_p}(\Sigma^2 - 2) + 2\gamma\Sigma(1-\phi_p)}{\sqrt{K_p}2(1+\Sigma\sqrt{\phi_p})} + \left(\frac{\Sigma}{\sqrt{K_p}} + \gamma\frac{(\phi_p - 1)\sqrt{\phi_p}\Sigma^2}{\sqrt{K_p}(1+\Sigma\sqrt{\phi_p})^2}\right)x + \mathcal{O}(x^2) \tag{57}$$

However, γ is of the order of x, therefore the second part of the first order term in x is a $\mathcal{O}(x^2)$. Adding Eqs. (56) and (57) it comes:

$$\frac{du_A}{dY} = U_\infty\left[-\frac{Y}{K_p} + \frac{\sqrt{\phi_p}(\Sigma^2 - 2) + 2\gamma\Sigma(1-\phi_p)}{\sqrt{K_p}2(1+\Sigma\sqrt{\phi_p})} + \mathcal{O}(x^2)\right] \tag{58}$$

The first order term in x vanishes. This explains why the choice of y_M hardly influences the macroscopic velocity profiles of our analysis in the free fluid channel.

References

[1] G.S. Beavers, D.D. Joseph, Boundary conditions at a naturally permeable wall, J. Fluid Mech. 30 (1967) 197–207.

[2] G.S. Beavers, E.M. Sparrow, B.A. Masha, Boundary conditions at a porous surface which bounds a fluid flow, AIChE J. 20 (1974) 596–597.

[3] W.P. Breugem, The influence of wall permeability on laminar and turbulent flows: theory and simulations, PhD thesis, Technische Universiteit Delft, 2005.

[4] W.P. Breugem, B.J. Boersma, R.E. Uittenbogaard, Direct numerical simulation of plane channel flow over a 3D cartesian grid of cubes, in: A.H. Reis, A.F. Miguel (Eds.), Proceedings of the Second International Conference on Applications of Porous Media, Evora Geophysics Center, Portugal, 2004, pp. 27–35.

[5] M. Chandesris, D. Jamet, Boundary conditions at a planar fluid–porous interface for a Poiseuille flow, Int. J. Heat Mass Transfer 49 (2006) 2137–2150.

[6] C. Deng, D.M. Martinez, Viscous flow in a channel partially filled with a porous medium and with wall suction, Chem. Eng. Sci. 60 (2) (2005) 329–336.

[7] D.A. Edwards, H. Brenner, D.T. Wasan, Interfacial Transport Processes and Rheology, Butterworth-Heinemann, 1991.

[8] A. Goharzadeh, A. Khalili, B.B. Jorgensen, Transition layer thickness at a fluid–porous interface, Phys. Fluids 17 (2005) 057102.

[9] B. Goyeau, D. Lhuillier, D. Gobin, M.G. Verlade, Momentum transport at a fluid–porous interface, Int. J. Heat Mass Transfer 46 (2003) 4071–4081.

[10] R.E. Larson, J.J.L. Higdon, Microscopic flow near the surface of two-dimensional porous media. Part 1. Axial flow, J. Fluid Mech. 166 (1986) 449–472.

[11] R.E. Larson, J.J. L Higdon, Microscopic flow near the surface of two-dimensional porous media. Part 2. Transverse flow, J. Fluid Mech. 178 (1987) 119–136.

[12] J.Y. Min, S.K. Kim, A novel methodology for thermal analysis of a composite system consisting of a porous medium and an adjacent fluid layer, J. Heat Transfer 127 (2005) 648–656.

[13] G. Neale, W. Nader, Practical significance of Brinkman's extension of Darcy's law: coupled parallel flows within a channel and a bounding porous medium, Can. J. Chem. Eng. 52 (1974) 475–478.

[14] D.A. Nield, The limitations of the Brinkman-Forchheimer equations in modeling flow in a saturated porous medium and at an interface, Int. J. Heat Fluid Flow 12 (3) (1991) 269–272.

[15] J.A. Ochoa-Tapia, S. Whitaker, Momentum transfer at the boundary between a porous medium and a homogeneous fluid – I. Theoretical development, Int. J. Heat Mass Transfer 38 (14) (1995) 2635–2646.

[16] J.A. Ochoa-Tapia, S. Whitaker, Momentum transfer at the boundary between a porous medium and a homogeneous fluid – II. Comparison with experiment, Int. J. Heat Mass Transfer 38 (14) (1995) 2647–2655.

[17] S. Richardson, A model for the boundary condition of a porous material. Part II, J. Fluid Mech. 49 (2) (1971) 327–336.

[18] P.G. Saffman, On the boundary condition at the surface of a porous medium, Stud. Appl. Math. L (2) (1971) 93–101.

[19] M. Sahraoui, M. Kaviany, Slip and no-slip velocity boundary conditions at interface of porous, plain media, Int. J. Heat Mass Transfer 35 (4) (1992) 927–943.

[20] S. Saleh, J.F. Thovert, P.M. Adler, Flow along porous media by partical image velocimetry, AIChE Journal 39 (11) (1993) 1765–1776.

[21] G.I. Taylor, A model for the boundary condition of a porous material. Part I, J. Fluid Mech. 49 (2) (1971) 319–326.

[22] S. Whitaker, Flow in porous media I: a theoretical derivation of Darcy's law, Transport Porous Media 1 (1986) 3–25.

[23] R.Kh. Zeytounian, Les modèles Asymptotiques de la mécanique des fluides I, Lecture Notes in Physics, Springer-Verlag, Berlin, 1986.

[24] D. Zwillinger, Handbook of Differential Equations, Academic Press, Boston, 1989.